Journal of Coordination Chemistry

ISSN: 0095-8972 (Print) 1029-0389 (Online) Journal homepage: https://www.tandfonline.com/loi/gcoo20

A kinetic study of the oxidation of hydroxamic acids by compounds I and II of horseradish peroxidase: Effect of transition metal ions

Uri Samuni, Eric Maimon & Sara Goldstein

To cite this article: Uri Samuni, Eric Maimon & Sara Goldstein (2018) A kinetic study of the oxidation of hydroxamic acids by compounds I and II of horseradish peroxidase: Effect of transition metal ions, Journal of Coordination Chemistry, 71:11-13, 1728-1737, DOI: 10.1080/00958972.2018.1493200

To link to this article: https://doi.org/10.1080/00958972.2018.1493200

© 2018 Informa UK Limited, trading as Taylor & Francis Group

Published online: 17 Oct 2018.

Submit your article to this journal

Article views: 407

View related articles

View Crossmark data

Citing articles: 1 View citing articles

Full Terms & Conditions of access and use can be found at
https://www.tandfonline.com/action/journalInformation?journalCode=gcoo20

JOURNAL OF COORDINATION CHEMISTRY
2018, VOL. 71, NO. 11-13, 1728–1737
https://doi.org/10.1080/00958972.2018.1493200

Taylor & Francis
Taylor & Francis Group

Check for updates

A kinetic study of the oxidation of hydroxamic acids by compounds I and II of horseradish peroxidase: Effect of transition metal ions

Eric Maimon[c], Uri Samuni[a,b] and Sara Goldstein[d]

[a]Chemistry & Biochemistry Department, Queens College, City University of New York, Flushing, NY, USA; [b]Ph.D. Programs in Biochemistry and Chemistry, The Graduate Center of the City University of New York, New York, NY, USA; [c]Chemistry Department, Ben-Gurion University, Beer-Sheva 84105 and Nuclear Research Centre Negev, Beer Sheva, Israel; [d]Institute of Chemistry, The Accelerator Laboratory, the Hebrew University of Jerusalem, Jerusalem, Israel

ABSTRACT

Oxidation of hydroxamic acids (HXs) generates HNO, and it is not clear whether it is formed also in the presence of metal ions. The kinetics of the oxidation of HXs, such as acetohydroxamic acid, suberohydroxamic acid, and suberoylanilide hydroxamic acid (SAHA), by compounds I and II of horseradish peroxidase (HRP) at pH 7.0 and 25 °C have been studied using rapid-mixing stopped-flow. The kinetics of these reactions were compared to those observed in the presence of $Cu(ClO_4)_2$, $NiSO_4$, or $ZnSO_4$. The rates decrease upon increasing $[Cu^{II}]$ at constant [HXs], and no oxidation of HX occurs when $[HX]/[Cu^{II}] \approx 2$, implying that HX oxidation in the presence of Cu^{II} proceeds through the free ligand since the predominant complex is CuX_2. In the case of Ni^{II}, the oxidation rate decreases upon increasing the ratio $[Ni^{II}]/[HX]$ beyond 1, where the predominant complex is $Ni^{II}X^+$, implying that its oxidation is feasible. The effect of Zn^{II} could be studied only on the rate of HXs oxidation by compound II demonstrating similar behavior to that of Ni^{II}. HXs were also oxidized catalytically by HRP/H_2O_2 at pH 7.0, demonstrating that metal ions facilitate the formation of HNO while hardly affecting its yield and the extent of HX oxidation.

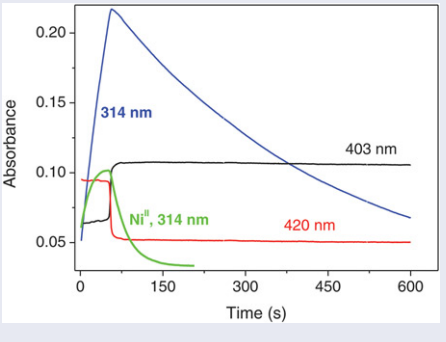

ARTICLE HISTORY
Received 6 February 2018
Accepted 14 May 2018

KEYWORDS
Acetohydroxamic acid; suberohydroxamic acid; SAHA; HRP; Cu^{II}; Ni^{II}; Fe^{III}; Zn^{II}; HNO

CONTACT Sara Goldstein sara.goldstein1@mail.huji.ac.il Institute of Chemistry, The Accelerator Laboratory, the Hebrew University of Jerusalem, Jerusalem 91904, Israel

© 2018 Informa UK Limited, trading as Taylor & Francis Group

1. Introduction

Redox-active metal ions and their organic complexes, specifically hydroxamic acids (RC(O)NHOH, HXs), play an important role in biological and catalytic processes. Their oxidation might take place at the metal center of the complex or the ligand, and the nature of the catalytic processes and any ensuing biological damage depend on the presence of transition metal ions. HXs have numerous biological and pharmacological activities, including (i) metal sequestration in treatment of iron overload and inhibition of metallo-enzymes such as ribonucleotide reductase and histone deacetylase [1, 2] and (ii) generation of reactive nitrogen species, such as acyl nitroso (RC(O)N = O), nitroxyl (HNO), nitric oxide (NO), and peroxynitrite under oxidative stress [2–7].

Previously, we studied the kinetics of the oxidation of acetohydroxamic acid (aceto-HX) and suberoylanilide hydroxamic acid (SAHA) by radiolytically borne radicals such as $^{\bullet}OH$, $^{\bullet}N_3$, and $CO_3^{\bullet-}$ [6, 7]. We have shown that one-electron oxidation of RC(O)NHOH forms the respective transient nitroxide radicals (RC(O)NHO$^{\bullet}$), which decompose bimolecularly forming HNO most probably through the formation of acyl nitroso (RC(O)N = O) as an intermediate [6, 7]. Therefore, it has been concluded that HXs under oxidative stress generate HNO, but might be also considered as NO-donors provided HNO oxidation is more efficient than its dimerization and dehydration forming nitrous oxide (N_2O) [8] or its reactions with other biological targets [9, 10]. Since HXs avidly chelate transition metal ions through the hydroxamate moiety [11, 12], the question raises whether HNO is formed also in the presence of transition metal ions.

2. Experimental

2.1. Materials

Water was purified using a Milli-Q purification system. All chemicals were of the highest available grade and used as received; acetohydroxamic acid (aceto-HX), suberohydroxamic acid (subero-HX), horseradish peroxidase (HRP, Type VI), (3-(*N*-morpholino) propanesulfonic acid (MOPS), and $Cu(ClO_4)\cdot 6H_2O$ were Sigma-Aldrich products. $FeCl_3\cdot 6H_2O$, $NiSO_4\cdot H_2O$, and $ZnSO_4\cdot 7H_2O$ were British Drug Houses (BDH) products. SAHA was purchased from LC Laboratories. H_2O_2 was obtained as a 30% solution from Merck. Stock solutions of 20 mM SAHA were prepared in DMSO. The solubility of SAHA and its oxidation products in water are relatively low, and therefore, the experiments were carried out using solutions containing 10–30% DMSO and were limited to relatively low [SAHA]. HRP was dissolved in water, and its concentration was determined spectrophotometrically using $\varepsilon_{403} = 100\,mM^{-1}cm^{-1}$ [13]. Compound II was prepared immediately before its use by adding 5 μM H_2O_2 to 5 μM HRP in 20 mM MOPS (pH 7.0) followed by the addition of 5.1 μM ferrocyanide. Compound II formation was evident by its typical Soret band at 420 nm and two absorption maxima at 527 and 556 nm [14]. Under our experimental conditions compound II decays slowly back to the native enzyme via a first-order reaction ($k = (5.7 \pm 0.1) \times 10^{-4}\ s^{-1}$ at 25 °C [15]).

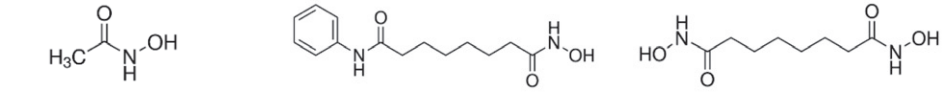

Figure 1. Structures of acetohydroxamic acid, SAHA, and suberohydroxamic acid.

2.2. Kinetics

Kinetic measurements at 25 °C were carried out using (i) an HP 8452A diode array spectrophotometer coupled with a thermostat (HP 89075C Programmable Multicell Transport) and (ii) a Bio SX-17MV Sequential Rapid-Mixing Stopped-Flow apparatus from Applied Photophysics having a 1 cm optical path. Rate constants of HX reactions with compounds I and II were determined using the Bio SX-17MV Sequential Stopped-Flow from Applied Photophysics with a 1 cm optical path. Compound I was formed *in situ* by mixing at a 1:1 concentrations ratio a solution of 5.1–5.2 μM HRP with a solution containing 5 μM H_2O_2 and excess concentrations of HX, i.e. [HX] ≫ [HRP]. HRP was added to H_2O_2 slightly over the stoichiometric amount to ensure that no recycling occurs due to any residual H_2O_2. The reduction of compound I to compound II by HX was followed at 411 nm, which is the isosbestic point for the spectra of HRP and compound II. Thus, any competition of compound II for any residual HX is excluded as a source of error. The subsequent reduction of compound II to HRP by HX was monitored at 422 nm where maximum absorbance change occurs between HRP and compound II. In some cases, preformed compound II ($\tau_{1/2} \asymp 20$ min) was mixed with an excess of HX and the reaction was monitored at 422 nm. An interference filter (420 nm, ASAHI SPECTRA CO) was used to minimize photochemistry from the Xe lamp. At least three independent experiments were performed for each experimental condition and the observed first-order rate constants (k_{obs}) represent an average of 3–5 measurements for each substrate concentration or pH. The bimolecular rate constants were derived from the dependence of k_{obs} on [HX].

2.3. Product analysis

(i) Initial and residual HX concentrations were assayed spectrophotometrically in acidic solutions and the presence of an excess of $FeCl_3$ by determining the formation of FeX^{2+} complex. Samples of reaction mixture (500–800 μL) were mixed with 30 mM $FeCl_3$ in 0.1 M HCl to a total volume of 1 mL, and the absorbance was read at 500 nm. The extinction coefficient has been reported to be $\asymp 1000n$ $M^{-1}cm^{-1}$ at pH $\asymp$ 2, where n is the number of the hydroxamate moieties bound per ferric ion [16–18]. Calibration curves were prepared using known concentrations of HX. The experiments were carried out using MOPS buffer since phosphate ions interfere with ferric and other metal ions binding to HXs.

2.4. Gas chromatography (GC)

HNO readily undergoes dimerization and dehydration forming N_2O [8], which can be assayed using GC. Sample solutions (7 mL) were placed in a glass vial (12 mL) sealed

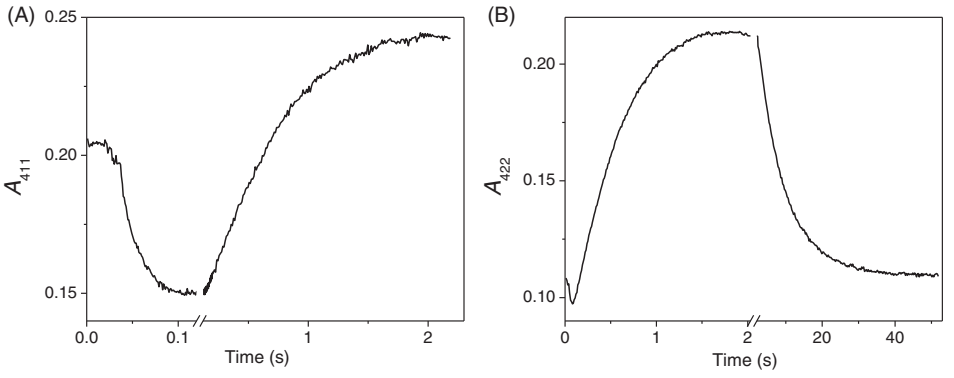

Figure 2. Kinetic traces monitored at 411 (A) and 422 nm (B) upon mixing a solution of 5.2 μM HRP in water with a solution of 5 μM H_2O_2 and 0.2 mM aceto-HX in 20 mM MOPS (pH 7.0) at a 1:1 ratio.

with a rubber septum. A gas aliquot of the reaction headspace (2 mL) was taken and 1 mL was injected at room pressure and temperature onto a 5890 Hewlett-Packard gas chromatograph equipped with a thermal conductivity detector, a 10 ft – 1/8 inch Porapak Q column at an operating oven temperature of 70 °C (injector and detector 150 °C) and a flow rate of 20 mL/min (He, carrier gas). The yields of N_2O were calculated on the basis of a standard curve prepared by injecting known amounts of N_2O gas (Maxima, Israel).

3. Results and discussion

The structures of HXs used in the present study are given in Figure 1. All experiments were carried out using MOPS buffer at pH 7.0 since phosphate ions interfere with metal binding and HX assay. Some experiments in the absence of metal ions were done using phosphate buffer (PB) demonstrating the same results in both buffers. Because of the low solubility of copper complexes of HXs in aqueous solutions, experiments requiring relatively high [Cu^{II}] were carried out in the presence of 30% DMSO.

3.1. Oxidation of HXs by HRP compounds I and II

HRP catalyzes the oxidation of a wide variety of compounds by H_2O_2. Peroxide reduction by HRP (R-$PorFe^{III}$) forms compound I (R-$^{+\bullet}PorFe^{IV}=O$), which is further reduced to compound II (R-$PorFe^{IV}=O$), and the catalysis normally proceeds via reactions 1–3, where X^- is a one-electron donor and $k_2 > k_3$ [19–22].

$$R{-}PorFe^{III} + H_2O_2 \rightarrow R{-}^{+\bullet}PorFe^{IV}=O + H_2O \quad k_1 = 1.7 \times 10^7 M^{-1}s^{-1}\ [23] \qquad (1)$$

$$R{-}^{+\bullet}\,PorFe^{IV}=O + X^- \rightarrow R{-}PorFe^{IV}=O + X^{\bullet} \qquad (2)$$

$$R{-}PorFe^{IV}=O + X^- + 2H^+ \rightarrow R{-}PorFe^{III} + X^{\bullet} + H_2O \qquad (3)$$

In the present study, we used compounds I and II for oxidizing HX, i.e. $X^- = RC(O)NHO^-$ and $X^{\bullet} = RC(O)NHO^{\bullet}$. The latter decomposes bimolecularly yielding

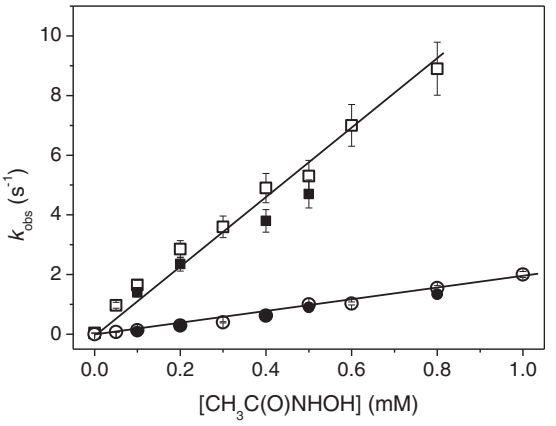

Figure 3. Oxidation of aceto-HX by compounds I and II. k_{obs} of $CH_3C(O)NHOH$ reaction with compound I (square symbols) and compound II (circle symbols) *vs.* [$CH_3C(O)NHOH$] in 20 mM MOPS (empty symbols) or in 20 mM PB (solid symbols) at pH 7.0.

RC(O)N = O, which readily reacts with nucleophiles generating HNO among other organic products [6, 7].

Upon mixing 5.1–5.2 μM HRP with 5 μM H_2O_2 and an excess of HX, the formation of compound I is completed within less than 0.2 s (reaction 1). The oxidation of HX by compound I (reaction 2) followed by oxidation of HX by compound II (reaction 3) were monitored at 411 nm and 422 nm, respectively (see "Experimental" section). Typical kinetic traces are shown in Figure 2, where Figure 2(A) shows the formation of compound I (completed within 0.2 s) and its reduction to compound II by 0.2 mM aceto-HX monitored at 411 nm. Figure 2(B) shows both the reduction of compound I to compound II and the subsequent reduction of compound II to HRP by 0.2 mM aceto-HX monitored at 422 nm. Note that the reduction of compound I to compound II by HX monitored at 411 nm is somewhat lower than that monitored at 422 nm due to some contribution of compound II reduction by HX (see "Experimental" section).

Both the formation rate of compound II via reaction 2 and its reduction rate to the native enzyme via reaction 3 obeyed first-order kinetics and the respective observed first-order rate constants ($k_{obs}(2)$ and $k_{obs}(3)$) depended linearly on $[HX]_o$ (Figure 3). The respective bimolecular rate constants derived from similar plots to those demonstrated in Figure 3 are summarized in Table 1. The same values were determined either in 20 mM PB or in 20 mM MOPS buffer (Figure 3). The k_3-value for HX oxidation by compound II is similar to that obtained by mixing preformed compound II with HX.

3.1.1. Effect of metal ions

The rates of compounds I and II reduction by HX decreased upon increasing [Cu^{II}] or [Ni^{II}] as indicated by the decrease in $k_{obs}(2)$ and $k_{obs}(3)$, respectively (Table 2).

The effect of Ni^{II} on the oxidation rates of HXs by compounds I and II is also presented as the dependence of $k_{obs}(2)/k_{obs}(2)_o$ and $k_{obs}(3)/k_{obs}(3)_o$ on [Ni^{II}]/[HX], where $k_{obs}(2)_o$ and $k_{obs}(3)_o$ are the respective values determined in the absence of Ni^{II} (Figure 4).

Table 1. k_2- and k_3-values at pH 7.0 and 25 °C.

HX	k_2, $M^{-1}s^{-1}$	k_3, $M^{-1}s^{-1}$
Aceto-HX	$(1.1 \pm 0.1) \times 10^4$	$(1.8 \pm 0.1) \times 10^3$
SAHA	$(2.4 \pm 0.2) \times 10^4$	$(5.2 \pm 0.1) \times 10^3$
Subero-HX	$(2.1 \pm 0.2) \times 10^4$	$(2.3 \pm 0.1) \times 10^3$

Table 2. Effect of [Cu^{II}] and [Ni^{II}] on the rate of compound I reduction by HX ($k_{obs}(2)$) and on the rate of compound II reduction by HX ($k_{obs}(3)$) in 10–20 mM MOPS buffer at pH 7.0.

HX	[HX], mM	Metal	[Metal], mM	$k_{obs}(2)$, s^{-1}	$k_{obs}(3)$, s^{-1}
Aceto-HX	0.8	–	–	9.2 ± 0.5	1.6 ± 0.1
		Ni^{II}	0.25	6.8 ± 0.6	1.12 ± 0.05
		Ni^{II}	0.5	5.6 ± 0.4	0.93 ± 0.07
		Ni^{II}	1	4.5 ± 0.4	0.75 ± 0.04
Aceto-HX	0.3	–	–	3.5 ± 0.3	0.40 ± 0.02
		Ni^{II}	0.3	2.3 ± 0.1	0.40 ± 0.01
		Ni^{II}	1	1.5 ± 0.1	0.25 ± 0.01
		Ni^{II}	2	1.1 ± 0.1	0.16 ± 0.01
		Ni^{II}	4	0.76 ± 0.05	0.10 ± 0.01
		Cu^{IIa}	0.15	1.7 ± 0.1	0.115 ± 0.005
		Cu^{IIa}	0.2	0.06 ± 0.01	2.6×10^{-3}
Subero-HX	0.2	–	–	4.1 ± 0.1	0.48 ± 0.02
		Ni^{II}	0.3	2.4 ± 0.1	0.40 ± 0.02
		Ni^{II}	0.5	2.0 ± 0.1	0.35 ± 0.01
		Ni^{II}	1	1.5 ± 0.1	0.25 ± 0.01
		Ni^{II}	2	1.1 ± 0.1	0.16 ± 0.01
		Ni^{II}	4	0.76 ± 0.05	0.10 ± 0.01
		Cu^{IIa}	0.1	1.3 ± 0.1	0.07 ± 0.01
		Cu^{IIa}	0.2	0.055 ± 0.005	4.9×10^{-3}
SAHA	0.2	–	–	5.1 ± 0.3	1.1 ± 0.1
		Ni^{II}	0.1	4.2 ± 0.3	0.88 ± 0.04
		Ni^{II}	0.5	3.3 ± 0.2	0.66 ± 0.02
		Ni^{II}	1	2.7 ± 0.1	0.52 ± 0.04
		Cu^{IIa}	0.05	2.8 ± 0.1	0.41 ± 0.03
		Cu^{IIa}	0.1	1.4 ± 0.1	0.14 ± 0.01
		Cu^{IIa}	0.125	0.07 ± 0.01	2.6×10^{-3}

[a]30% DMSO. In the absence of metal ions the values determined for $k_{obs}(2)$ and $k_{obs}(3)$ do not differ from those obtained in the absence of DMSO.

Neither compound I nor compound II of all HXs tested was observed in the presence of Zn^{II} or Fe^{III} even at low concentrations, thus excluding the possibility of studying their effects. Instead, an alternative strategy was adopted where preformed compound II was reacted with HX and Zn^{II} or Fe^{III}. Figure 5 demonstrates the dependence of $k_{obs}(3)/k_{obs}(3)_o$ on [Zn^{II}]/[HX] in the case of aceto-HX, subero-HX, and SAHA. In the case of Fe^{III}, even this strategy could not be employed because the reaction is too fast for accurate measurement using the rapid-mixing stopped-flow technique. For example, the reaction of $\asymp 2\,\mu M$ preformed compound II with 300 μM aceto-HX and 12.5 μM Fe^{III} resulted in $k_{obs}(3) \asymp 23\,s^{-1}$, i.e. $k_3 \asymp 2.3 \times 10^6\ M^{-1}s^{-1}$.

Of the metal ions tested, Fe^{III} forms the most stable hydroxamato complexes, followed by Cu^{II} and $Ni^{II} \asymp Zn^{II}$ at a decreasing order [17, 18, 24, 25]. Also, at high ratios of [aceto-HX] to [metal] the predominant complex at pH 7.0 is CuX_2 [17] whereas for Ni^{II} about 60% is NiX^+, 30% NiX_2 and the rest NiX_3^- [25]. SAHA yields a tris-hydroxamato complex in the case of Fe^{III} and bis-hydroxamato complexes in the case of Cu^{II}, Ni^{II}, and Zn^{II}, both in the solid state and in solution [18]. Subero-HX forms a 1:1 stoichiometry of metal:ligand with Fe^{III}, Cu^{II}, Ni^{II}, and Zn^{II}, but also a 2:3 metal:ligand stoichiometry in neutral solutions except with Cu^{II} [24]. Nevertheless, the results

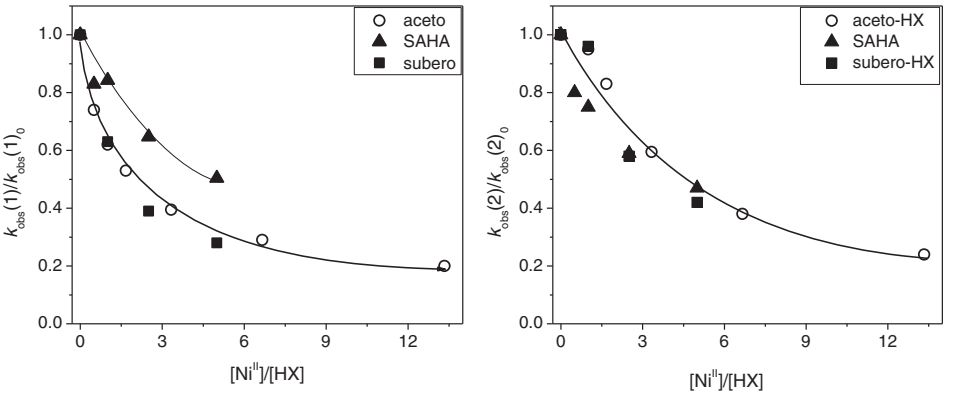

Figure 4. Effect of [Ni^{II}] on the rates of HX oxidation by compounds I and II. Dependence of $k_{obs}(2)/k_{obs}(2)_o$ (left) and $k_{obs}(3)/k_{obs}(3)_o$ (right) on [Ni^{II}]/[HX] in the presence of 0.3 mM aceto-HX, 0.2 mM SAHA or subero-HX, and 10-20 mM MOPS at pH 7.0. $k_{obs}(2)_o$ and $k_{obs}(3)_o$ are the respective values determined in the absence of Ni^{II}.

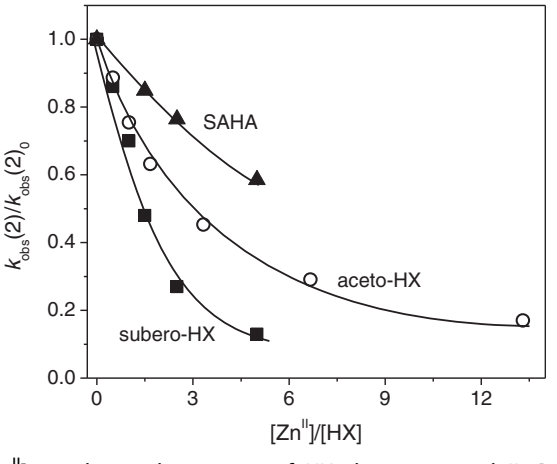

Figure 5. Effect of [Zn^{II}] on the oxidation rate of HXs by compound II. Dependence of $k_{obs}(3)/k_{obs}(3)_o$ on [Zn^{II}]/[HX] in the presence of 0.3 mM aceto-HX and 0.2 mM SAHA or subero-HX in 10–20 mM MOPS at pH 7.0.

demonstrate that the effect of Cu^{II} is different from those of Ni^{II} and Zn^{II}. The rates of the oxidation of all tested HXs by both compounds I and II decrease as [Cu^{II}] increases, and no HX oxidation takes place when [HX]/[Cu^{II}] $\asymp$ 2. Therefore, we conclude that oxidation of HXs in the presence of Cu^{II} proceeds through the free ligand alone, since the main complex at pH 7.0 is CuX_2. In the case of Ni^{II} and Zn^{II} the oxidation rates decrease significantly when [HX]/[metal] $>$ 1. However, the oxidation still proceeds under limiting concentrations of HX where the predominant complex is expected to be NiX^+ or ZnX^+, implying that the latter have free access to compounds I and II.

3.2. Effect of metal ions on the catalytic oxidation of HX by HRP/H_2O_2

Previously, it has been demonstrated that HRP in the presence of H_2O_2 catalyzes the formation of HNO from hydroxyurea [26]. Our results show that HRP alone does not

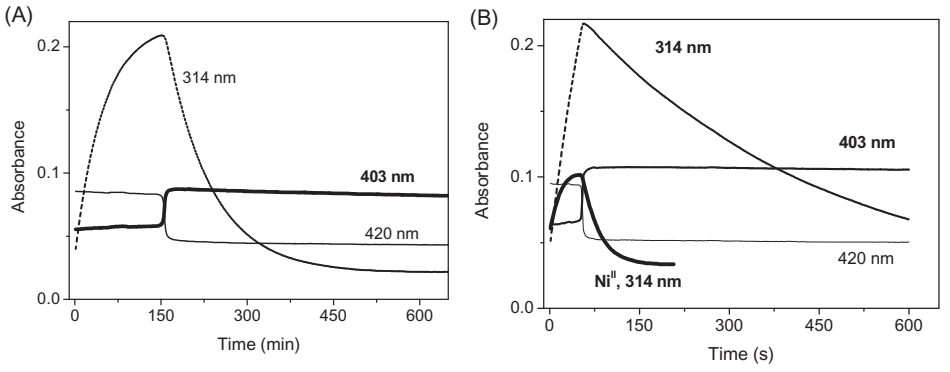

Figure 6. Spectral changes monitored at 314, 403, and 420 nm during the catalytic oxidation of (A) 1 mM aceto-HX by 200 μM H_2O_2 and 1 μM HRP at pH 7.0 (40 mM PB); (B) 400 μM SAHA by 100 μM H_2O_2 and 1 μM HRP at pH 7.0 (20 mM MOPS, 15% DMSO) in the absence and presence of 20 μM Ni^{II} . The kinetic traces at 403 and 420 nm are the same with and without Ni^{II}.

react with HX, but upon addition of H_2O_2 ($[H_2O_2] \gg [HRP]$), the oxidized heme species observed is compound II (λ_{max} at 420 nm), which upon complete consumption of H_2O_2 returns back to the native enzyme (λ_{max} at 403 nm). Typical kinetic traces are shown for the oxidation of 1 mM aceto-HX by 200 μM H_2O_2 and 1 μM HRP at pH 7.0 (Figure 6(A)) and for the oxidation of 0.4 mM SAHA by 100 μM H_2O_2 and 1 μM HRP at pH 7.0 (Figure 6(B)). During the catalytic process, a transient species with maximum absorbance at 314 nm is accumulated (Figure 6), presumably the previously invoked acyl nitroso [6, 7]. Upon complete consumption of H_2O_2 this transient decays via a first-order reaction and its respective k_{obs} increased linearly upon increasing [HX] (results not shown). Similar kinetic profiles were observed in the case of subero-HX. The periods required for complete consumption of H_2O_2 differed among different HXs since reaction 3 is the rate-determining step and the reaction of each HX has its own rate constant (Table 1).

The presence of Cu^{II}, Ni^{II}, or Zn^{II}, even at relatively low concentrations, increased the rate of A_{314} decay thus decreasing the extent of its maximal accumulation as demonstrated in the presence of Ni^{II} (Figure 6(B)), which could not be detected at higher [metal].

Gas samples from the reaction mixture headspace were collected for determination of N_2O, which is a marker for HNO formation, i.e. $[N_2O] = 2\,[HNO]$. The results summarized in Table 3 demonstrate that the effect of the metal ions on N_2O yield is insignificant.

The extent of HX oxidation was determined under the conditions where $[HX]_o > 2[H_2O_2]_o$, demonstrating that Δ[HX] increased linearly with $[H_2O_2]_o$. A ratio $\Delta[HX]/[H_2O_2]_o = 1.5 \pm 0.1$ was determined for aceto-HX and SAHA and 0.75 ± 0.05 for subero-HX, which is a dihydroxamic acid, i.e. 1.5 ± 0.1 per hydroxamate moiety. The effect of the metal ions on the extent of HX oxidation is summarized in Table 4, demonstrating that the peroxidative process is hardly affected by the presence of the metal ions except for Fe^{III} and subero-HX.

Table 3. Yields of N_2O generated during HX oxidation by HRP (1–1.6 μM) and H_2O_2 at pH 7.0 (20 mM PB or MOPS). The error is ±10%.

HX	[HX], mM	[H_2O_2], μM	Metal	[Metal], μM	[N_2O], μM
Aceto-HX	1	300	–	–	112
		300	Cu^{II}	20	131
		150	Cu^{II}	20	71
		300	Ni^{II}	100	120
		300	Fe^{III}	100	99
		300	Fe^{III}	250	105
SAHA	0.4	150	–	–	41
		150	Cu^{II}	20	54
		150	Ni^{II}	100	62
		150	Fe^{III}	100	49

Table 4. Effects of metal ions on the extent of HX depletion measured upon HX oxidation by H_2O_2 catalyzed by 1 μM HRP in aerated solutions at pH 7.0 (20 mM MOPS).

HX	[HX], mM	[H_2O_2], mM	Metal	[Metal], mM	Δ [HX], mM[a,b]
Aceto-HX	1				
	1	0.2	–	–	0.31
	1	0.2	Cu^{II}	0.02	0.32
	1	0.2	Ni^{II}	0.2	0.31
	1	0.2	Ni^{II}	0.5	0.27
	1	0.2	Zn^{II}	0.4	0.34
	1	0.2	Zn^{II}	2	0.26
	0.5	0.2	–	–	0.27
	0.5	0.2	Fe^{III}	0.15	0.22
	0.5	0.2	Fe^{III}	0.5	0.23
	0.5	0.2	Fe^{III}	2	0.19
SAHA	0.4	0.1	–	–	0.14
	0.4	0.1	Cu^{II}	0.02	0.14
	0.4	0.1	Ni^{II}	0.04	0.14
Subero-HX	0.5	0.2	–	–	0.30
	0.5	0.2	Cu^{II}	0.02	0.32
	0.5	0.2	Ni^{II}	0.2	0.26
	0.5	0.2	Ni^{II}	1	0.28
	0.5	0.2	Zn^{II}	1	0.32
	0.5	0.2	Zn^{II}	5	0.24
	0.5	0.2	Fe^{III}	0.4	0.26
	0.5	0.2	Fe^{III}	0.7	0.10
	0.5	0.2	Fe^{III}	1	0.12

[a]The error is ±10%.
[b]Δ[HX] per hydroxamate moiety.

4. Conclusion

The present results demonstrate that: (i) the rate constants of HXs oxidation by compound I are higher than those by compound II; (ii) these rate constants decrease upon increasing the concentration of metal ions to the extent that depends on the metal itself. The effect of Cu^{II} is different from those of Ni^{II} and Zn^{II} and is attributable to the predominant complex formed at pH 7.0. The oxidation is prevented when [HXs]/[Cu^{II}] $\asymp$ 2, implying that it proceeds through the free ligand. In the case of Ni^{II} and Zn^{II} the oxidation rates decreased upon increasing the ratio [metal]/[HX] beyond 1, implying that oxidation of the 1:1 complex is feasible; (iii) catalytic oxidation of HXs by HRP/H_2O_2 at pH 7.0 generates HNO through formation of the corresponding presumed acyl nitroso intermediates absorbing at 314 nm; (iv) the metal complexes facilitate the decomposition of acyl nitroso compounds while hardly affecting the yield of HNO and

the extent of HX oxidation. It is concluded that HX under oxidative stress generates HNO, which is not prevented but rather accelerated by a variety of transition metal ions.

Acknowledgment

Dedicated to Professor Dan Meyerstein on the occasion of his 80th birthday.

Disclosure statement

No potential conflict of interest was reported by the authors.

Funding

This work has been supported by the Pazy Foundation, Grant number 276/18.

References

[1] E.M.F. Muri, M.J. Nieto, R.D. Sindelar, J.S. Williamson. *Curr. Med. Chem.*, **9**, 1631 (2002).
[2] P. Kovacic, C.L. Edwards. *J. Recept. Signal Transduct. Res.*, **31**, 10 (2011).
[3] M.T. Gladwin, J.H. Shelhamer, F.P. Ognibene, M.E. Pease-Fye, J.S. Nichols, B. Link, D.B. Patel, M.A. Jankowski, L.K. Pannell, A.N. Schechter, G.P. Rodgers. *Br. J. Haematol.*, **116**, 436 (2002).
[4] S.B. King. *Curr. Med. Chem.*, **10**, 437 (2003).
[5] M.J. Burkitt, A. Raafat. *Blood*, **107**, 2219 (2006).
[6] S. Goldstein, A. Samuni. *J. Phys. Chem. A*, **115**, 3022 (2011).
[7] Y. Samuni, D.A. Wink, M.C. Krishna, J.B. Mitchell, S. Goldstein. *Free Radic. Biol. Med.*, **73**, 291 (2014).
[8] V. Shafirovich, S.V. Lymar. *Proc. Natl. Acad. Sci. USA*, **99**, 7340 (2002).
[9] J.M. Fukuto, C.H. Switzer, K.M. Miranda, D.A. Wink. *Annu. Rev. Pharmacol. Toxicol.*, **45**, 335 (2005).
[10] C.H. Switzer, W. Flores-Santana, D. Mancardi, S. Donzelli, D. Basudhar, L.A. Ridnour, K.M. Miranda, J.M. Fukuto, N. Paolocci, D.A. Wink. *Biochim. Biophys. Acta*, **1787**, 835 (2009).
[11] B. Kurzak, H. Kozlowski, E. Farkas. *Coord. Chem. Rev.*, **114**, 169 (1992).
[12] R. Codd. *Coord. Chem. Rev.*, **252**, 1387 (2008).
[13] K.G. Paul, T. Stigbrand. *Acta Chem. Scand.*, **24**, 3607 (1970).
[14] S.A. Adediran, A.M. Lambeir. *Eur. J. Biochem.*, **186**, 571 (1989).
[15] A. Samuni, E. Maimon, S. Goldstein. *Biochim. Biophys. Acta*, **1861**, 2060 (2017).
[16] S.J. Barclay, B.H. Hanh, K.N. Raymond. *Inorg. Chem.*, **23**, 2011 (1984).
[17] E. Farkas, E. Kozma, M. Petho, K.M. Herlihy, G. Micera. *Polyhedron*, **17**, 3331 (1998).
[18] D.M. Griffith, B. Szocs, T. Keogh, K.Y. Suponitsky, E. Farkas, P. Buglyo, C.J. Marmion. *J. Inorg. Biochem.*, **105**, 763 (2011).
[19] B. Chance. *Arch. Biochem. Biophys.*, **41**, 416 (1952).
[20] P. George. *Biochem. J.*, **54**, 267 (1953).
[21] H.B. Dunford, J.S. Stillman. *Coord. Chem. Rev.*, **19**, 187 (1976).
[22] H.B. Dunford. *Prog. React. Kinet. Mech.*, **38**, 119 (2013).
[23] D. Dolman, G.A. Newell, M.D. Thurlow, H.B. Dunford. *Can. J. Biochem.*, **53**, 495 (1975).
[24] E. Farkas, E.A. Enyedy, H. Csoka. *Polyhedron*, **18**, 2391 (1999).
[25] E. Farkas, E.A. Enyedy, H. Csoka. *J. Inorg. Biochem.*, **79**, 205 (2000).
[26] J.M. Huang, E.M. Sommers, D.B. Kim-Shapiro, S.B. King. *J. Am. Chem. Soc.*, **124**, 3473 (2002).